High-Q nanoring surface plasmon microresonator

Chang-Ling Zou,[1] Yun-Feng Xiao,[2] Zheng-Fu Han,[1,3] Chun-Hua Dong,[1] Xiang-Dong Chen,[1] Jin-Ming Cui,[1] Guang-Can Guo,[1] and Fang-Wen Sun[1,4]

[1]*Key Laboratory of Quantum Information, University of Science and Technology of China, Hefei 230026, China*
[2]*State Key Lab for Mesoscopic Physics, School of Physics, Peking University, Beijing 100871, China*
[3]*e-mail: zfhan@ustc.edu.cn*
[4]*e-mail: fwsun@ustc.edu.cn*

Received August 24, 2010; accepted September 18, 2010;
posted September 28, 2010 (Doc. ID 133678); published November 16, 2010

We investigate whispering-gallery-like surface plasmon modes in a silver nanoring located on a diamond substrate. These hybrid modes are demonstrated to possess not only high quality factors (several hundred), but also ultra-small mode area as well as ultra-small mode volume (less than 0.1 μm^3). In experiments, this cavity structure shows great potential for studying a strong and deterministic coherent interaction between the hybrid mode and single quantum system embedded in the substrate. © 2010 Optical Society of America

OCIS codes: 140.3945, 240.6680.

1. INTRODUCTION

The coherent interaction between photons and emitters has attracted much attention for more than thirty years [1], because it plays a central role in many applications, especially for cavity quantum electrodynamics and quantum information processing. A strong light–matter interaction is usually required, as it essentially depends on the field intensity at the emitter position. Optical microresonators have been employed recently as a platform for realizing such strong coupling and are characterized by two physical parameters: quality factor (Q) and mode volume (V). Dielectric microcavities have been studied extensively with quality factors Q up to millions [2,3]. Alternatively, the metal surface plasmon (SP) resonators with low Q but ultrasmall mode volume are emerging recently.

As a natural plasmon resonator, silver nanowire (nanocylinder) [4,5] has been investigated, as it shows potential applications in single photon sources [6] and quantum information science [7]. However, it basically suffers from low Q factor (less than 100) because of end surface scattering. High Q factor is expected in the rotational symmetric SP microresonator. Recently, Min *et al.* [8] experimentally demonstrated SPP modes with Q above 1000 in a silver-coated microdisk, and Xiao *et al.* [9] have numerically investigated hybrid ring-type microresonators with $Q>400$ and small mode volume ($\sim 0.1\ \mu m^3$). In addition to these, silver nanorings have been successfully synthesized with a very smooth surface, where the SP wave can travel along the cavity surface with a very low scattering loss [10,11]. These show potential in SP amplification by stimulated emission of radiation (SPASER) [12,13]. In this paper, we numerically investigate whispering-gallery (WG)-like SP modes in a silver nanoring that is placed on a diamond substrate. These hybrid modes are demonstrated to possess not only high Q (several hundred) but also ultrasmall mode volume (less than 0.1 μm^3). From the experimental point of view, this cavity structure shows great potential for studying light–matter interaction, especially for deterministic coupling between cavity and single emitters, since the nanoring can be manipulated by other nanostructures, such as nanotips.

2. RESULTS AND DISCUSSION

The proposed nanoring is shown in Fig. 1(a). It can be chemically synthesized with principal radius r_p ranging from 2 to 10 μm and minor radius r_d ranging from 20 to 100 nm [10,11]. Here we adapt the ideal ring model with a circular cross section and smooth surface (thus no scattering loss). Similar to other plasmon resonators, the silver nanoring supports plasmon modes propagating along its surface. Because of the rotational symmetry, the field distribution of the plasmon mode can be described by $E(r,z)\cos(im\phi)$, where $2m$ denotes the number of nodes along the ring surface.

In experiments, the silver nanoring is placed on a substrate, which provides a convenient platform for studying the plasmon mode stably coupling to selected emitters (quantum dots or fluorescence molecules) buried in the substrate. Here, a smooth diamond film with $n_{sub}=2.4$ is especially chosen as the substrate, as single nitrogen-vacancy (NV) defect centers are included therein. The transition of the NV defect has a zero-phonon line at 637 nm. NV centers have been widely studied for cavity quantum electrodynamics and quantum information because they have a long-lived spin triplet in their electronic ground states [14,15] that can be initialized, manipulated, and read out through highly stable optics and microwaves at room temperature.

To investigate the mode property, here we numerically obtain the eigenmodes of the nanoring by the full-vectorial finite element method [16]. The Q factor is obtained by $Q=\mathrm{Re}(\omega)/2\,\mathrm{Im}(\omega)$, where ω is the solved complex eigenfrequency. The mode volume is defined as the ratio of total energy and the peak energy [17], $V \equiv \int w\,\mathrm{d}^3x/\max(w)$, where $w=[\mathrm{d}\varepsilon(\vec{r})/\mathrm{d}\omega|E|^2+\mu_0|H|^2]/2$ is

 © 2010 Optical Society of America

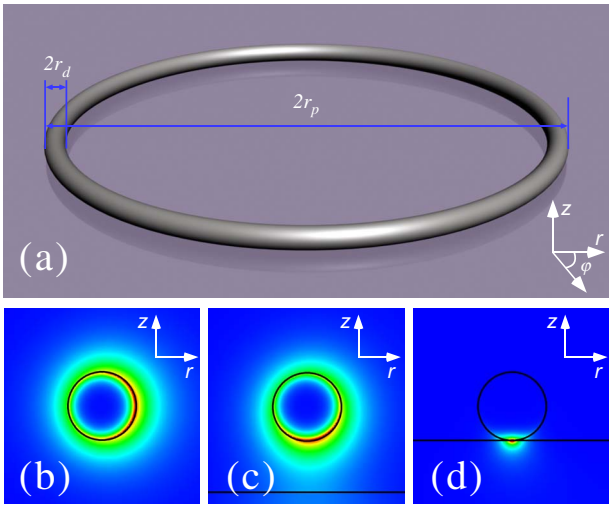

Fig. 1. (Color online) (a) Schematic of a silver nanoring on diamond substrate. The geometry of the nanoring is defined by the principal radius r_p and minor radius r_d. (b), (c), (d) Energy density distribution on the cross section of nanoring with $r_p=5$ μm and $r_d=80$ nm at $\phi=0$; gaps between nanoring and the diamond substrate are g,,$=\infty$, 150 nm, and 0, respectively.

the energy density [18]. Here, E and H are the electric and magnetic fields; $\varepsilon=-19.2-0.19i$ and 1 are the electric permittivities of silver and air, respectively, at 637 nm and room temperature; and μ_0 is the vacuum magnetic permeability.

The energy distribution profiles of the WG-like plasmon modes in the (r,z) plane are shown in Figs. 1(b)–1(d) for different nanoring–substrate gaps: $g=\infty$, 150 nm, and 0. When the silver nanoring is far away from the substrate, i.e., it is in an isotropic environment surrounded by air, the mode field is mirror-symmetric with respect to axis r [Fig. 1(b)]. Different from straight nanowire, the field is stronger at the outer surface for the nanoring as a result of the curvature geometry. By moving the nanoring close to the substrate, the plasmon modes are found to be strongly attracted by the high-index substrate [Fig. 1(c)], as a result of the non-isotropic environment. When the nanoring–substrate gap decreases to zero, the plasmon mode propagates along the nanoring–dielectric interface, as shown in Fig. 1(d).

The mode properties can be characterized by an effective index defined as $n_{eff}=(c/r_p)[\mathrm{d}m/\mathrm{d}\,\mathrm{Re}(\omega)]$. For $r_p=5$ μm and $r_d=80$ nm, the effective indices for the modes in Figs. 1(b)–1(d) are about 1.013, 0.999, and 2.43, respectively. When the silver nanoring begins to approach the substrate, n_{eff} extraordinarily decreases at first. In fact, this decrease is a result of the reduction of the actually effective radius of the modes [Fig. 1(c)] as the coupling between the plasmon mode and traveling wave in the substrate invokes the characteristics of the hybrid mode. With further decreasing of the gap, the field overlap between them increases exponentially, and n_{eff} then switches to increasing. In this process, the quality factor of the mode also exhibits a strong decrease at first and then increases. This kind of transition can be understood by the mode coupling between the plasmon mode and traveling modes in the substrate. Unlike the pure plasmon mode confined at the metal surface, the traveling modes in the substrate have no confinement, and the mode energy is strongly dissipated. The coupling between them forms the hybrid mode.

The calculated Q and V of the nanoring in air and on the substrate are plotted in Fig. 2 by fixing the minor radius $r_d=80$ nm. To understand the behavior of the Q factor, we introduce the loss mechanism of WG-like SP modes as $1/Q_{total}=1/Q_{rad}+1/Q_{abs}$. The Q_{rad} and Q_{abs} describe the optical radiation loss and metal absorption loss, respectively. No scattering loss is included in our consideration, since the surface of the nanoring could be improved in experiments. In addition, the absorption of surrounding material is also ignored, as this loss could be tiny compared to that of metal. Bending could lead to radiation, so the Q_{total} is limited by radiation at small radius r_p, as we can see from Fig. 1(b), where the maximum of the field is on the outer surface. With increasing of the principal radius, the radiation Q_{rad} increases. When Q_{rad} exceeds Q_{abs}, the nanoring goes into the absorption limited regime. The absorption can be estimated by $Q_{abs}=1/\eta\times\mathrm{Re}(\varepsilon)/\mathrm{Im}(\varepsilon)$ where η is the portion of energy confined in the metal. For a nanoring in air, the Q_{air} reaches its maximum 450 at about $r_p=5$ μm. However, the Q does not reach its maximum even for $r_p=10$ μm. This is because Q_{rad} is smaller when the nanoring is on the substrate, as analyzed above. There is always nearly 70% energy confined in the substrate and 20% energy confined in the nanoring, corresponding to $Q_{abs}\approx 500$.

Figure 2(b) shows the mode volume with different r_p. The mode profile is almost the same for different principal radii, which induces the linear increase of mode volume with the length of the ring, i.e., proportional to r_p. However, the V for nanoring on substrate is almost 1/10 of that in air. This is the result of the small contraction area of the hybrid structure and the high index of the substrate.

Note that despite the larger radiation loss due to bending when r_p is small (less than 5 μm), the Q factor is still larger than for nanowire, benefiting from the round geometry without end face scattering. When $r_p=2$ μm, the corresponding nanowire length is 12.6 μm, and our simula-

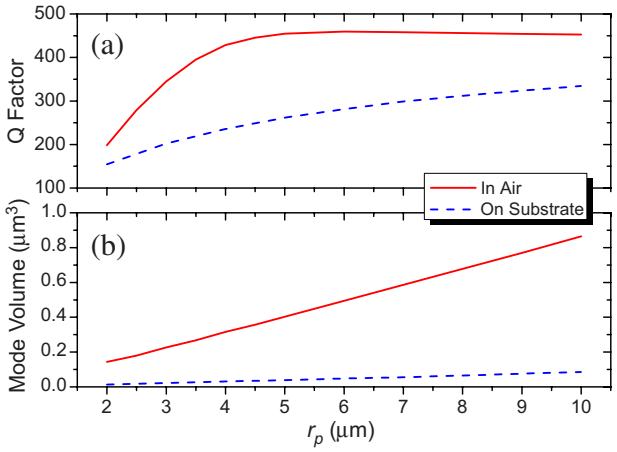

Fig. 2. (Color online) (a) Q factor and (b) mode volume of the modes with nanoring in air (solid curve) and on the diamond substrate (dashed curve). The minor radius $r_d=80$ nm, and the wavelength in the simulations is 637 nm, corresponding to the transition of NV centers.

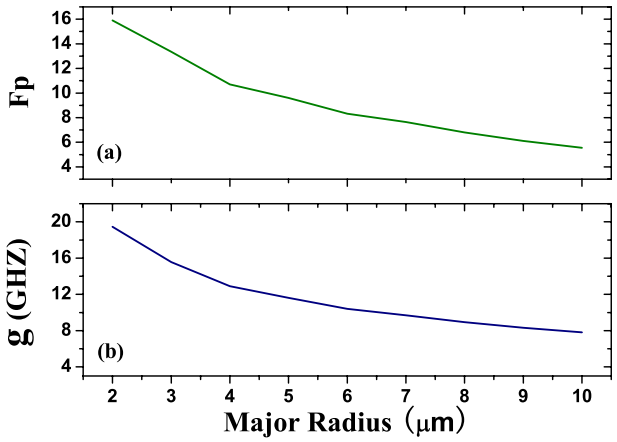

Fig. 3. (Color online) Calculated Purcell factor (a) and coupling strength (b) of NV center at the peak field intensity, with fixed r_d=80 nm and wavelength of 637 nm.

tion of the SP modes of nanowire shows its Q factor is only 64, about 1/2.5 of that of the nanoring in air.

We now study the hybrid plasmon mode coupled to NV centers in the diamond substrate. Although the Q of a nanoring on substrate is only half of that in air, the nanoring on substrate has much smaller V. The enhancement of the spontaneous emission can be approximately described by the Purcell factor $F_p=3Q(\lambda/n)^3/(4\pi^2V)$ [19]. It is worth noting that the F_p provides only a rough estimation of the radiative decay rate, and the non-resonant channels could also be included in a more rigorous study [20]. As shown in Fig. 3(a), the Purcell factor F_p is largest when $r_p=2$ μm. In addition to the enhanced spontaneous emission of the emitter near the nanoring benefiting from the large bandwidth of the plasmon mode, the silver nanoring is also suitable for coupling to multipole emitters, especially to artificial quantum dots that have large spectral range. For coupling with single NV centers, the coupling strength is $g=d\sqrt{\hbar\omega/2\varepsilon V}/\hbar$, corresponding to the vacuum Rabi frequency. The coupling strength for various r_p is shown in Fig. 3(b). For example, the nanoring with $r_p=5$ μm has the maximal coupling strength $g_{\max}=11.6$ GHz with $d=2.74\times10^{-29}$ C ·m, the dipole moment of the NV center transition. A number of NV centers could lead to a large coupling effect and gain [21].

The silver nanoring provides a new type of microcavity for coherent light–matter coupling experiments. The silver nanoring on the substrate can be easily moved and manipulated by a nanotip. Thus, it provides an excellent method and platform for deterministic coupling between cavity and single NV centers, or between other emitters in substrates for the scanning cavity microscope technique [22]. It is still possible to deterministically couple two or more different single emitters through the nanoring. In addition, a nanoring with a Q factor of a few hundred and ultra-small mode volume is comparable to a diamond microdisk with Q=100 [23] and a photonic crystal microcavity with Q=585 [24].

3. CONCLUSION

In conclusion, we investigated and analyzed the WG-like plasmon modes in a nanoring. Benefiting from the symmetric ring shape, the radiation limited cavity Q factor is up to a few hundred, much higher than nanowires. In addition, the mode volume of the SP modes in a nanoring on a substrate is ultra-small. It will give rise to strong modification of the emission properties of emitters in substrates, and also large coupling strength between SP modes and emitters. These give the nanoring potential for use as a SPASER [12,13] and in studies of the fundamental physics of cavity quantum electrodynamics [25,26].

ACKNOWLEDGMENTS

The work was supported by the National Fundamental Research Program of China under Grant No. 2006CB921900, the Knowledge Innovation Project of Chinese Academy of Sciences, and the National Natural Science Foundation of China (NSFC) (Grant Nos. 60621064, 60537020). F. W. S. is also supported by the new faculty starting funds from University of Science and Technology of China (USTC) and the Fundamental Research Funds for the Central Universities. Y. F. X. is supported by the Research Fund for the Doctoral Program of Higher Education (No. 20090001120004) and the Scientific Research Foundation for the Returned Overseas Chinese Scholars.

REFERENCES AND NOTES

1. H. J. Kimble, "The quantum internet," Nature **453**, 1023–1030 (2008).
2. K. J. Vahala, "Optical microcavities," Nature **424**, 839–846 (2003).
3. C.-H. Dong, F.-W. Sun, C.-L. Zou, X.-F. Ren, G.-C. Guo, and Z.-F. Han, "High-Q silica microsphere by poly(methyl methacrylate) coating and modifying," Appl. Phys. Lett. **96**, 061106 (2010).
4. H. Ditlbacher, A. Hohenau, D. Wagner, U. Kreibig, M. Rogers, F. Hofer, F. R. Aussenegg, and J. R. Krenn, "Silver nanowires as surface plasmon resonators," Phys. Rev. Lett. **95**, 257403 (2005).
5. R. Kolesov, B. Grotz, G. Balasubramanian, R. J. Stohr, A. A. L. Nicolet, P. R. Hemmer, F. Jelezko, and J. Wrochtrup, "Wave-particle duality of single surface plasmon polaritons," Nat. Phys. **5**, 470–474 (2009).
6. D. E. Chang, A. S. Sorensen, P. R. Hemmer, and M. D. Lukin, "Quantum optics with surface plasmons," Phys. Rev. Lett. **97**, 053002 (2006).
7. G.-P. Guo, Z.-R. Lin, T. Tu, H.-O. Li, C.-L. Zou, X.-F. Ren, and G.-C. Guo, "Quantum bus of metal nanowire with surface plasmon polaritons," http://arxiv.org/abs/0904.3603.
8. B. Min, E. Ostby, V. Sorger, E. Ulin-Avila, L. Yang, X. Zhang, and K. Vahala, "High-Q surface plasmon-polariton whispering-gallery microcavity," Nature **457**, 455–458 (2009).
9. Y.-F. Xiao, B.-B. Li, X. Jiang, X. Hu, Y. Li, and Q. Gong, "High quality factor, small mode volume, ring-type plasmonic microresonator on a silver chip," J. Phys. B **43**, 035402 (2010).
10. H. M. Gong, L. Zhou, X. R. Su, S. Xiao, S. D. Liu, and Q. Q. Wang, "Illuminating dark plasmons of silver nanoantenna rings to enhance exciton-plasmon interactions," Adv. Funct. Mater. **19**, 298–303 (2009).
11. L. Zhou, X.-F. Fu, L. Yu, X. Zhang, X. F. Xu, and Z.-H. Hao, "Crystal structure and optical properties of silver nanorings," Appl. Phys. Lett. **94**, 153102 (2009).
12. D. J. Bergman and M. I. Stockman, "Surface plasmon amplification by stimulated emission of radiation: Quantum generation of coherent surface plasmons in nanosystems," Phys. Rev. Lett. **90**, 027402 (2003).
13. Z.-J. Yang, N.-C. Kim, J.-B. Li, M.-T. Cheng, S.-D. Liu, Z.-H. Hao, and Q.-Q. Wang, "Surface plasmons amplifications in

single Ag nanoring," Opt. Express **18**, 4006–4011 (2010).
14. T. A. Kennedy, J. S. Colton, J. E. Butler, R. C. Linares, and P. J. Doering, "Long coherence times at 300 K for nitrogen-vacancy center spins in diamond grown by chemical vapor deposition," Appl. Phys. Lett. **83**, 4190–4192 (2003).
15. T. Gaebel, M. Domhan, I. Popa, C. Wittmann, P. Neumann, F. Jelezk, J. R. Rabeau, N. Stavrias, A. D. Greentree, S. Prawer, J. Meijer, J. Twamley, P. R. Hemmer, and J. Wrachtrup, "Room-temperature coherent coupling of single spins in diamond," Nat. Phys. **2**, 408–413 (2006).
16. M. Oxborrow, "Traceable 2-D finite-element simulation of the whispering-gallery modes of axisymmetric electromagnetic resonators," IEEE Trans. Microwave Theory Tech. **55**, 1209–1217 (2007).
17. Here, we adopt the peak value of energy outside the ring for the nanoring in air, and the peak value in the substrate when the nanoring is on the substrate.
18. R. F. Oulton, V. J. Sorger, D. A. Genov, D. F. P. Pile, and X. Zhang, "A hybrid plasmonic waveguide for subwavelength confinement and long range propagation," Nat. Photonics **2**, 496–500 (2008).
19. J.-M. Gerard and B. Gayral, "Purcell effect for InAs quantum boxes in three-dimensional solid-state microcavities," J. Lightwave Technol. **17**, 2089 (1999).
20. A. F. Koenderink, "On the use of Purcell factors for plasmon antennas," http://arxiv.org/abs/1007.1074.
21. M. Ambati, D. A. Genov, R. Oulton, and X. Zhang, "Active plasmonics: surface plasmon interaction with optical emitters," IEEE J. Sel. Areas Commun. **14**, 1395–1403 (2008).
22. D. Englund, B. Shields, K. Rivoire, F. Hatami, J. Vuckovic, H. Park, and M. D. Lukin, "Deterministic coupling of a single nitrogen vacancy center to a photonic crystal cavity," Nano Lett. **10**, 3922–3926 (2010).
23. C. F. Wang, Y.-S. Choi, J. C. Lee, E. L. Hu, J. Yang, and J. E. Butler, "Observation of whispering gallery modes in nanocrystalline diamond microdisks," Appl. Phys. Lett. **90**, 081110 (2007).
24. C. F. Wang, R. Hanson, D. D. Awschalom, E. L. Hu, T. Feygelson, J. Yang, and J. E. Butler, "Fabrication and characterization of two-dimensional photonic crystal microcavities in nanocrystalline diamond," Appl. Phys. Lett. **91**, 201112 (2007).
25. V. V. Temnov and U. Woggon, "Superradiance and subradiance in an inhomogeneously broadened ensemble of two-level systems coupled to a low-Q cavity," Phys. Rev. Lett. **95**, 243602 (2005).
26. D. E. Gomez, K. V. Vernon, P. Mulvaney, and T. J. Davis, "Surface plasmon mediated strong exciton–photon coupling in semiconductor nanocrystals," Nano Lett. **10**, 274–278 (2010).